duced form of hDAAO with buffer solutions equilibrated at increasing oxygen concentration: the time course of absorbance change at 455 nm is monophasic. A reoxidation rate constant of 1 x 10^4 $M^{-1}s^{-1}$ was calculated.

The combination of steady state and pre–steady state measurements indicates that hDAAO follows a ternary complex (sequential) kinetic mechanism (k_{diss} is too slow to belong to the kinetic mechanism), and that the kinetic parameters are in the same order of magnitude of those determined for the pig kidney DAAO (the main difference is represented by the rate of flavin reduction which is 20–fold slower in the human enzyme, see Table 1).

Interaction between hDAAO and pLG72.

At first we focused on the demonstration of the interaction between pLG72 and hDAAO. This interaction was investigated by means of gel permeation chromatography: a fixed amount of pLG72 (25 nmoles) was added of increasing concentrations of hDAAO (from 5 to 200 nmoles). The elution volume of hDAAO was shifted from 14.1 ml to 8.1 ml, i.e., from a dimeric to a polymeric oligomerization state. The maximal amount of hDAAO shifted to this polymeric state was observed at a hDAAO:pLG72 ratio between 4:1 and 8:1 (see Fig. 2). The addition of 0.1 % sarcosyl (a detergent required for the solubilization of pGL72) to hDAAO did not affect its elution volume, as well as no change in elution volume of yeast DAAO was observed following the addition of pLG72.

The physical association between pLG72 and DAAO has been further confirmed by far Western blot, differential scanning calorimetry and plasmon resonance (BIAcore) experiments.

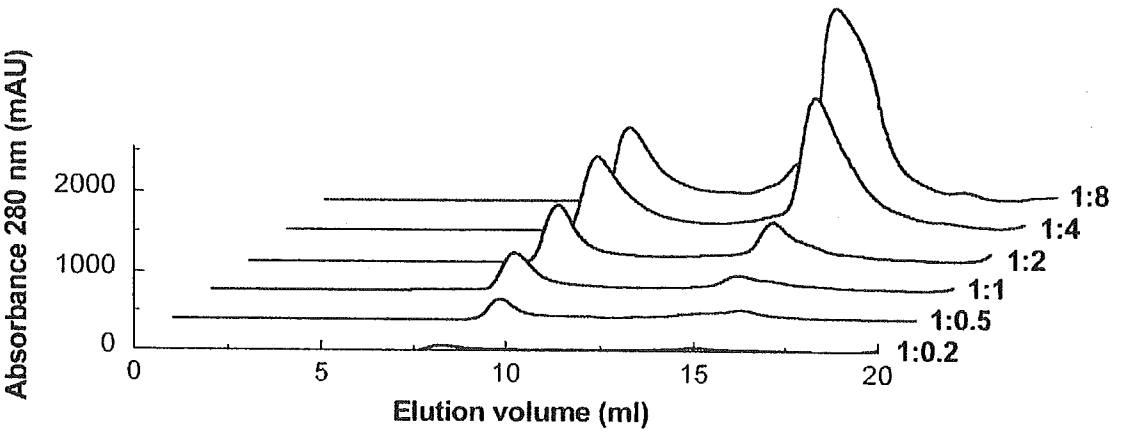

Fig. 2. Analysis by gel–permeation chromatography of interaction between pLG72 and hDAAO. A fixed amount of pLG72 (25 nmoles) was added of increasing concentrations of hDAAO (5 nmoles–200 nmoles).

Conclusions

Schizophrenia is a psichosys that affects nearly 1 % of people around the world and accounts for about 2.5 % of health–care costs. The expression in fairly large amount of hDAAO as a stable and active holoenzyme, the definition of its properties, and the demonstration of the specific interaction with pLG72 paves the way to the elucidation of the effect of pLG72 on the stability and on the kinetics of the reaction catalyzed by

the flavoprotein DAAO in human brain. Furthermore, the availability of the pGL72-DAAO protein complex in solution and under physiological conditions, together with measurements to track functional and structural changes, will represent an ideal system for finding small molecules that inhibit and/or modulate protein–protein interactions.

Acknowledgements

This work was supported by grants from Italian MIUR *(Prot 2004058243)*, from FAR to M. S. Pilone and L. Pollegioni, and from Fondazione CARIPLO to L. Pollegioni.

References

1 Schell, M. J., Molliver, M. E., Snyder, S. H. (1995) *Proc. Natl. Acad. Sci. U S A.* **92**, 3948–3952.
2 Mothet J. P., Parent, A. T., Wolosker, H., Brady, R. O., Linden, D. J., Ferris, C. D., Rogawski M. A., Snyder, S. H. (2000) *Proc. Natl. Acad. Sci. U S A.* **97**, 4926–4931.
3 Chumakov, I. *et al.* (2002) *Proc. Natl. Acad. Sci. U S A* **99**, 13675–13680.
4 Raibekas, A. A. *et al.* (2000) *Proc. Natl. Acad. Sci. U S A* **97**, 3089–3093.
5 Massey (1991) In *Flavins and Flavoproteins*, pp. 59–66, Walter de Gruyter & Co., Berlin.
6 Pilone, M. S. (2000) *Cell. Mol. Life Sci.* **57**, 1732–1747.
7 Hashimoto, A. and Oka, T. (1997) *Progr. Neurobiol.* **52**, 325–353.

Crystal Structures of Wild-type and R181M L-Lactate Oxidase from Aerococcus viridans

Kazuko Yorita[1], Yasufumi Umena[2,5], Takeshi Matsuoka[3], David P. Ballou[4], Makoto Abe[2], Akiko Kita[2,6], Tomitake Tsukihara[5], Yukio Morimoto[2,6], and Kiyoshi Fukui[1]

[1]Institute for Enzyme Research, University of Tokushima, Tokushima, Japan.
[2]Research Reactor Institute, Kyoto University, Osaka, Japan.
[3]Fine Chemicals & Diagnostics Division, Asahi Kasei Pharma, Shizuoka, Japan.
[4]Department of Biological Chemistry, University of Michigan Medical School, Ann Arbor, MI, USA.
[5]Institute for Protein Research, Osaka University, Osaka, Japan.
[6]RIKEN, Harima Institute at Spring-8, Hyogo, Japan.

Introduction

L-Lactate oxidase from *Aerococcus viridans* (LOX) belongs to the α-hydroxyacid-oxidizing (α-HAO) flavoprotein family (*1*). The mechanisms of the respective reductive half-reactions for a series of α-hydroxyacid substrates within this enzyme family represent one of the central interests. We have already shown that Arg181 and Arg268 of L-lactate oxidase have crucial roles in both α-hydroxyacid substrate binding and flavin reduction in the catalytic sequence (*2,3*). These two Arg residues are conserved in all members of the α-HAO enzyme family, and are located in proximity to the FMN in the active site (*4-12*). We have solved the crystal structures of both wild-type and R181M mutant forms of LOX in the absence of substrates, inhibitors, or activators at resolutions of 2.1 Å (wild-type) and 2.13 Å, (R181M).

Experimental Procedures

Purification methods of wild-type and R181M LOX were described previously (*3*). The enzymes were passed through a Sephacryl S-200HR (Amersham Biosciences) column prior to the crystallization (*13*). Either hanging-drop or sitting-drop vapor-diffusion methods were used in the presence of PEG8000 at 25 °C. X-ray diffraction data were collected with the MAR CCD detector using synchrotron radiation at beam-line BL41XU of SPring-8, Japan. The wavelength was 1 Å and the crystal-to-detector distance was 200 or 130 mm. A total of 180 frames were collected with 1° oscillation and 5 sec exposures. Molecular replacement using the coordinates of glycolate oxidase (PDB code 1GOX) as the model was carried out to solve the structures of R181M LOX. The wild-type structure was solved by molecular replacement with R181M LOX as the model. Programs used were DENZO, CCP4, CNS, XtalView, SHELEX and PyMOL.

Results and Discussion

Statistics for the data collection and refinement of wild-type and R181M LOX are summarized in Table 1. The crystal packing of wild-type and R181M LOX were same, and the asymmetric unit was found to be a tetramer with 64 monomers in a unit cell. Solvent contents were in the normal range for globular proteins. Each monomer structure was solved independently. Because of the bulky side chain of Tyr-374 at the C-terminus, and its positioning in the center of tetramer, the mobility of the C-terminus

is less than that of the other members of the α-HAO family; thus, the structure of complete C-terminal as well as the N-terminal domains could be solved (Fig. 1a).

Each monomer of wild-type and R181M LOX is a typical $(\beta/\alpha)_8$-TIM barrel. Only the disordered region between residues #202 – #213 and #205 – #216 for R181M and wild-type, respectively, were not determined (Fig. 1b). The *si*-face of the FMN isoalloxazine ring is oriented toward the center of the $(\beta/\alpha)_8$-barrel, and the *re*-face is in contact with the hydrophobic β-strand. These characteristics of the LOX tertiary structure are conserved in other α-HAO family members, such as glycolate oxidase (*5*), flavocytochrome b_2 (*6*), a soluble chimeric form of L-mandelate dehydrogenase (*11*), and

Table 1: Data Collection and Refinement Statistics

	Wild-type	R181M
	Crystallographic Data	
Space group	*I* 422	*I* 422
Unit cell parameters (a,b,c)	191.096, 191.096, 194.497	192.632, 192.632, 200.263
Z	64	64
*V*m (Å ^{3}/Da)	2.71	2.84
Resolution range (Å)	500–2.07	500–1.80
No. of observed reflections	1,391,263	1,745,892
No. of unique reflections	108,566	162,003
Completeness	100	99.8
Redundancy	12.8	10.8
R_{merge} [d] (%)	14.2	13.7
	Refinement Statistics	
Resolution range (Å)	500–2.1	500–2.13
Total number of reflections used	104,057	104,168
No. of reflections in working set	98,834	98,953
No. of reflections in test set	5,223	5,215
R_{work} (%)	22.26	21.23
R_{free} (%)	25.66	24.64
No. of protein non-H atoms	11,216	11,216
No. of polypeptide chains	4	4
Number of FMN atoms	124	124
No. of water molecules	642	603
Rms deviations Bond lengths (Å)	0.006688	0.006430
Bond angles (deg)	1.14817	1.09075

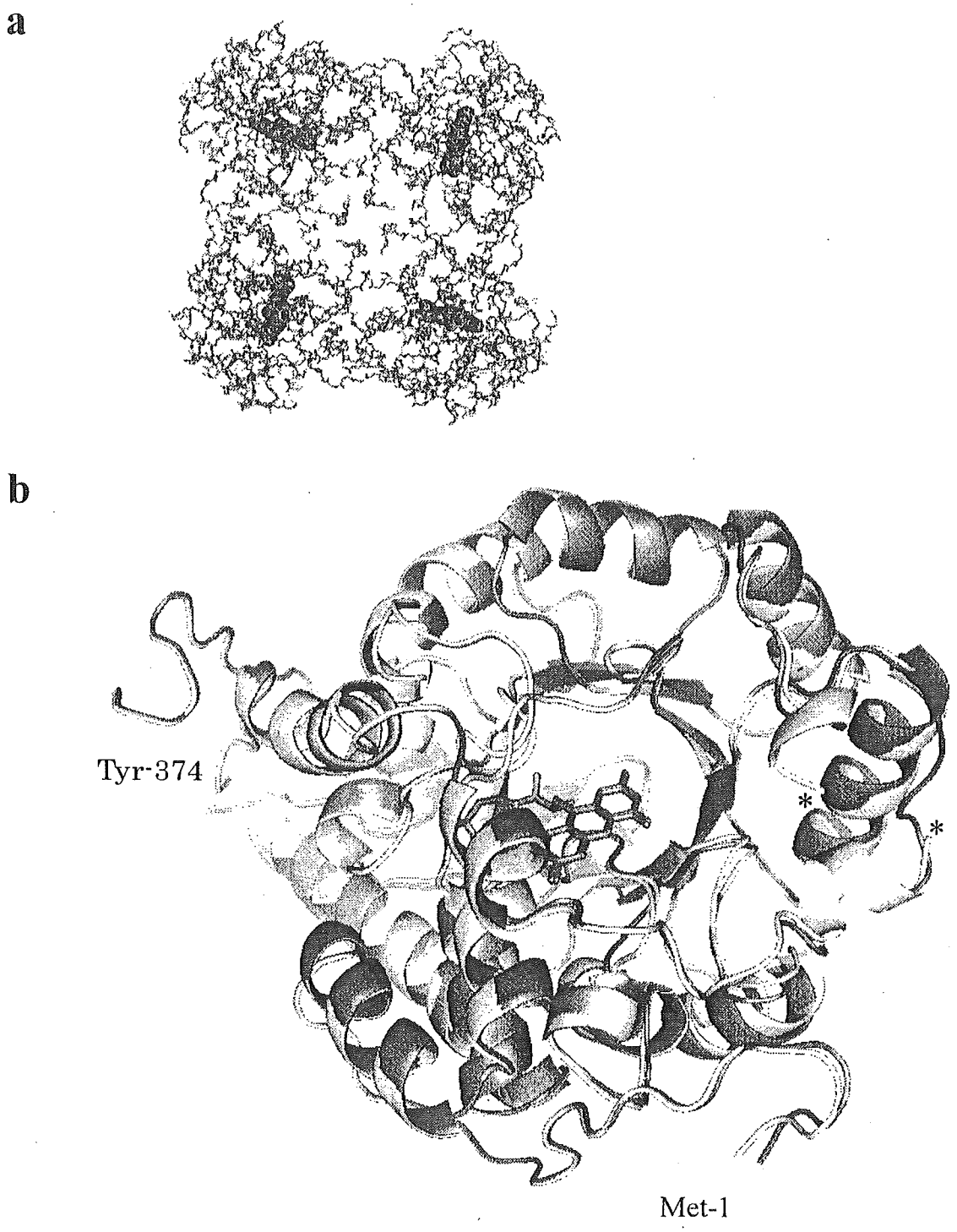

Fig. 1. Quarternary and tertiary structures of wild-type and R181m LOX. (a) One tetramer in the asymmetric unit was observed both in wild-type (*bold stick*) and in R181M (*thin line*) LOX. Only the main chain structures are described with the prosthetic groups of FMN (*dotted sphere*). (b) Cartoons of the monomer structures of wild-type (*black*) and R181M (*white*) LOX. *Asterisks* indicate the disordered structures, #202 –#213 and #205–#216 for R181M and wild-type, respectively.

recently, long chain α-hydroxy acid oxidase (*12*). Within the region containing the conserved amino acid residues near the FMN, the topology of Arg-181 and Arg-268 with respect to FMN in wild-type LOX is different from that seen in glycolate oxidase, and in long chain α-hydroxy acid oxidase.

B-Factors of main- and side-chains in R181M and wild-type LOX are shown in Fig. 2. The mobility of the main chains is same in wild-type and in R181M LOX, but most of the side chain mobility is slightly larger in R181M than in the wild-type. Two exceptions were observed at Arg-268 and Tyr-124. The side chains of these two residues show distinctly more mobility in wild-type LOX than in R181M LOX. This resulted in the orientations of the side-chain guanidinium groups of Arg-268, the side-chain phenyl groups of Tyr-124, and the main-chain carbonyl groups of Ala-95 being different in the active sites of wild-type and R181M LOX (Fig. 3).

Our previous results that described the kinetic and spectral characteristics of LOX showed that Ala-95, Arg-18,1 and Arg-268 of LOX are important for the reductive half reaction with the substrate L-lactate (*3,14*). Tyr-124 of LOX is far from the FMN and located at the entrance of the channel to FMN (Fig. 3). The corresponding residue of

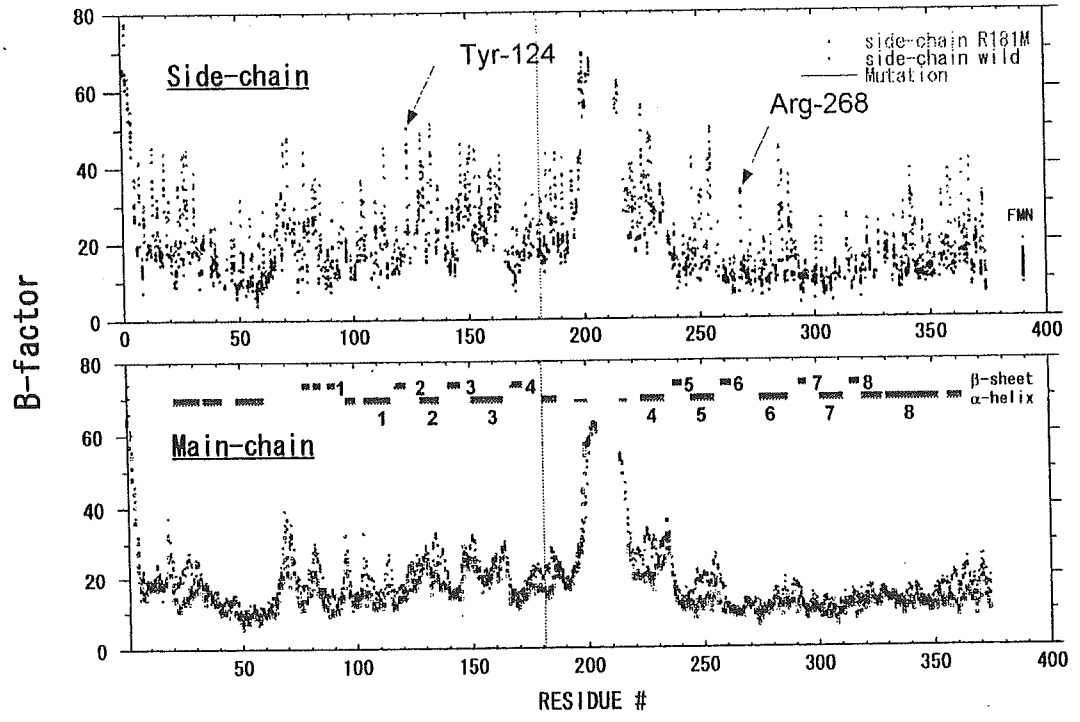

Fig. 2. B-Factors of main- and side-chain of wild-type (*circle*) and R181M (*triangle*) LOX. Only the side-chains of Tyr-124 and Arg-268 are more mobile in wild-type than in R181M. Line at the residue number 181 indicated the mutation position. Components of the $(\beta/\alpha)_8$-barrel were also indicated in the figure.

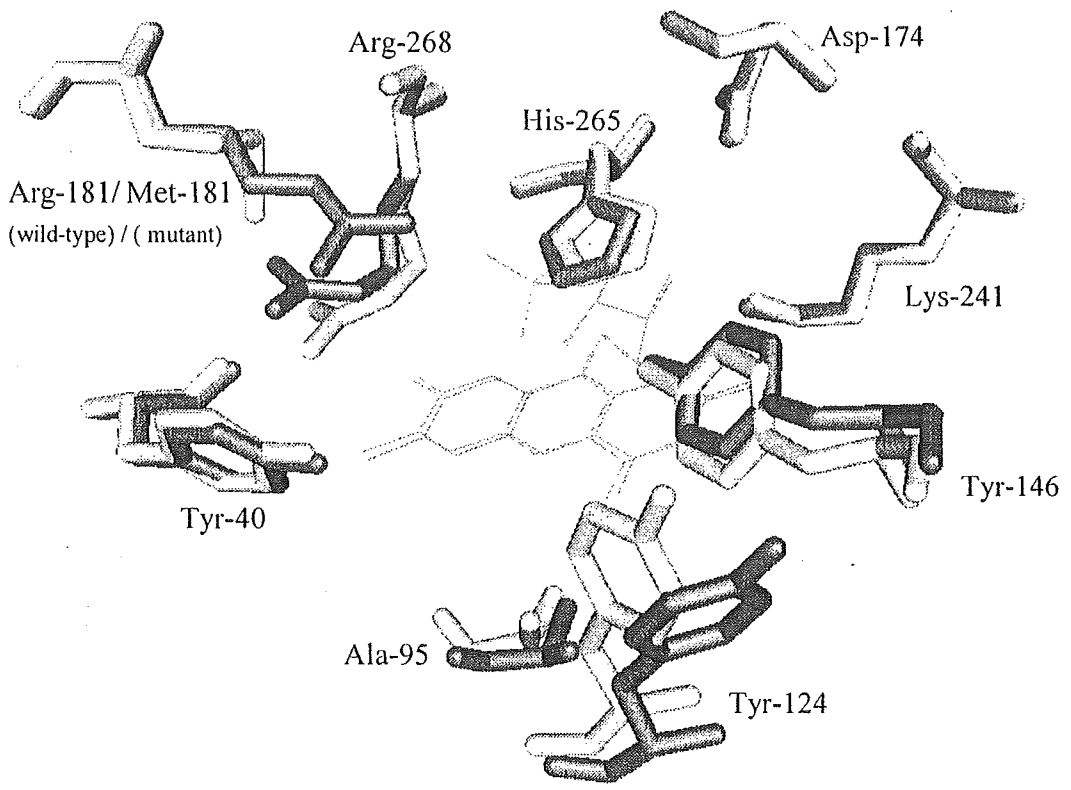

Fig. 3. Active site topologies of wild-type and R181M LOX. Whole structures of wild-type and R181M LOX were superimposed by the program CCP4. Orientation of the side-chains of Arg-268 and Tyr-124 are distinctly different in wild type (*black*) than in R181M (*white*) LOX.

glycolate oxidase is the more bulky Trp-108 (*5*). Less mobility in R181M LOX may reflect changes of the dynamic structure around the active site; therefore, the different orientations of these residues can block the entry and the stability of substrates in the active site of the mutant R181M. Moreover, Arg-289 of flavocytochrome b_2, which corresponds to Arg-181 of LOX, has been reported to show two different conformations in the sulfite adduct crystal structure; one is stacked against Arg-376 side chain (corresponds to Arg-268 of LOX), and the other is pointed toward the active site (*15*). In R181M LOX without any effectors, the guanidinium group of Arg-268 orientates towards the FMN isoalloxazine-ring and has less mobility (Fig. 3). The results of our previous kinetic and spectral studies combined with these structural determinations of wild-type and R181M LOX, permit us to interpret the functional role of Arg-181 in terms of concerted actions with Arg-268 both in binding of the substrate L-lactate and in stabilization of the transition state in the dehydrogenation of the substrate.

Acknowledgements
This work was partly supported by a Grant-in-Aid (to Y.M.) for the National Project on Protein Structural and Function Analysis from the Ministry of Education, Culture, Sports, Science and Technology of Japan and by the United States Public Health Service Grant GM 11106 (to V.M. and D.P.B.).

References

1. Maeda-Yorita, K., Aki, K., Sagai, H, Misaki, H., & Massey, V. (1995) *Biochimie* **77**, 631-642.
2. Yorita, K, Janko, K., Aki, K., Ghisla, S., Palfey, B. & Massey, V. (1997) *Proc. Natl. Acad. Sci. USA* **94**, 9590-9595.
3. Yorita, K, Matsuoka, T., Misaki, H. & Massey, V. (2000) *Proc. Natl. Acad. Sci. USA* **97**, 13039-13044.
4. Lindqvist, Y. & Branden, C.I. (1989) *J. Biol. Chem.* **264**, 3624-3628.
5. Lindqvist, Y. (1989) *J. Mol. Biol.* **209**, 151-166.
6. Xia, Z.X. & Mathews, F.S. (1990) *J. Mol. Biol.* **212**, 837-863.
7. Ghisla, S. & Massey, V. (1991) In: Chemistry and Biochemistry of Flavoenzymes, Vol 2 (Muller F. ed.) CRC Press, Boca Raton, FL., pp243-289
8. Le, K.H.D. & Lederer, F. (1991) *J. Biol. Chem.* **266**, 20877-20881.
9. Lederer, F. (1991) In: Chemistry and biochemistry of flavoenzymes, Vol 2 (Muller F. ed.) CRC Press, Boca Raton, FL., pp153-242
10. Smekal, O., Yasin, M., Fewson, C.A., Reid, G.A. & Chapman, S.K. (1993) *Biochem. J.* **290**, 103-107
11. Sukumar , N., Xu, Y., Gatti, D.L., Mitra, B. & Mathews, F.S. (2001) *Biochemistry* **40**, 9870-9878.
12. Cunane, L.M., Barton, J.D., Chen, Z-w, Le, K.H.D., Amar, D, Lederer F. & Mathews, F.S. (2001) *Biochemistry* **44**, 1521-1531.
13. Umena, Y., Yorita, K., Matsuoka, T., Abe, M., Kita, A., Fukui, K., Tsukihara, T. and Morimoto, Y., 2005) *Acta Cryst.* F61, 439-441.
14. Yorita, K, Aki, K., Ohkuma-Soejima, T., Kokubo, T. & Massey, V. (1996) *J. Biol. Chem.* **271**, 28300-28305.
15. Tegoni, M. & Cabbillau, C. (1994) *Protein Sci.* **3**, 303-313.

H265Q L-Lactate Oxidase from *Aerococcus viridans*

Kazuko Yorita[1], Takeshi Matsuoka[2], David P. Ballou[3] and Kiyoshi Fukui[1]

[1]Institute for Enzyme Research, University of Tokushima, Tokushima, Japan.
[2]Fine Chemicals & Diagnostics Division, Asahi Kasei Pharma, Shizuoka, Japan.
[3]Department of Biological Chemistry, University of Michigan Medical School, Ann Arbor, MI 48109-0606, USA

Introduction

The wide variety of functions of flavoproteins is thought to result from the tuning of flavin reactivity by interactions with the surrounding amino acid residues in the active sites. FMN enzymes catalyzing the oxidation of L-α-hydroxy acids have been found to share remarkable similarities in properties, making it likely that they constitute a family of proteins with common structural motifs. The most thoroughly characterized members of this family are yeast lactate dehydrogenase (flavocytochrome b_2) and L-lactate monooxygenase from *M. Smegmatis* (*1,2*). Other members are glycolate oxidase, long chain α-hydroxy acid oxidase and L-mandelate dehydrogenase (*3-5*). The crystal structures of flavocytochrome b_2, glycolate oxidase, a soluble chimeric form of L-mandelate dehydrogenase with a portion of glycolate oxidase, and recently, a long chain α-hydroxy acid oxidase, were solved by X-ray diffraction methods. They all showed similar protein folding patterns, with a typical $(\beta/\alpha)_8$-TIM barrel arrangements as well as several conserved amino acid residues around the FMN in the active center. (*6-9*).

L-Lactate oxidase from *Aerococcus viridans* (LOX) belongs to the α-hydroxy-acid-oxidizing flavoprotein family (*10*). This enzyme is a soluble simple flavoprotein, and catalyzes the oxidation of the most common α-hydroxy acid, L-lactate, to pyruvate and hydrogen peroxide. Non-enzymatic hydrolysis reaction of pyruvate to acetate and carbon dioxide is not detected with L-lactate oxidase. These enzymatic characteristics are powerful to work on the reaction mechanisms of the reductive half reaction and also the recognition mechanism of the family members by the substrate α-hydroxy acids. We had already shown that two conserved arginine residues, Arg-181 and Arg-268, in the active site of LOX are crucial for the reductive half reaction (*11*).

His265 of L-lactate oxidase is also conserved in all members of this family and believed to be an important residue for the reduction of the enzyme by α-hydroxyacids. This histidine residue is assumed to abstract a proton from α-hydroxy acids to form a carbanion. In this work the importance of His265 on the reaction mechanism of the reductive half reaction was tested with the H265Q variant of L-lactate oxidase.

Experimental Procedures

A simple and rapid PCR mutational method (*12*) was used to construct the His265 to Gln point mutation of wild-type L-lactate oxidase from *Aerococcus viridans* (H265Q LOX). In this method, a pair of primers was designed in inverted tail-to-tail directions to amplify the cloning vector together with the target sequence, but one of the primers had a corresponding nucleotide replacement at the desired position for the mutation. PCR cocktail solution was prepared with 1 μM each of the primers, 200 μM each of

dNTPs, one unit of Ex Taq polymerase (Takara), 6 μg of the full length of pAOX8 (~5.6 kbp), which encodes the target gene for wild-type LOX, as the template DNA and 10x Ex Taq Buffer in 50 μl volume solution. Primers are 5'-AGTTGACGAGCACCTT GGTTAGATA-3' and 5'-ATATGAAGCTCCAGGTTCATTTGAC-3'. After pre-incubation at 96 °C for 5 min, 30 cycles of PCR at 94 °C for 1 min, 63 °C for 1 min and 72 °C for 4 min were done in 50 μl of PCR cocktail solution. PCR product was purified from agarose gel with QIAEX II agarose gel extraction kit (Qiagen) and was self-ligated by Takara BKL kit (Takara), followed by use for transformation of One Shot INVαF' competent cell (Invitrogen). DNA sequencing analysis of this construct in *E. coli* confirmed the point mutation of H265Q and no other mutations in the full length of LOX gene, and this system was directly used for the large scale culture in TB media for 44 hours at 37 °C. Purification procedures are similar as for wild-type and other mutant forms; we also omitted the acetone extraction step (*10*).

Circular dichroism (CD) spectra and fluorescence spectra were recorded at 25 °C with a Jasco J-820 spectrophotometer, and Hitachi 650-60 fluorescence photometer, respectively. Stopped-flow procedures for rapid reaction kinetics and other spectral experiments were done as described previously (*10,13,14*).

Results

Kinetic characterization of H265Q LOX

The kinetic parameters for the oxidative- and reductive- half reactions and the sulfite binding- and releasing-reaction of H265Q, wild-type and five other mutants, where Arg-181 and/or Arg-268 was mutated to Lys or Met, were summarized in Table 1. The rate for the reoxidation reaction of the reduced form of H265Q with molecular oxygen was 3.4×10^5 $M^{-1}sec^{-1}$, only one fifth that of wild-type enzyme. On the other hand, the reductive half reaction of H265Q by the substrate L-lactate showed second-order kinetics with a rate constant of 0.01 $M^{-1}sec^{-1}$ at 25 °C, pH 7.0. This rate constant is 10^8–fold less than that for wild-type enzyme under the same conditions. Other variants where Arg-181 or Arg-268 is mutated to either Lys or Met, had decreased efficiency in the reductive half reaction, but none of mutants had less activity than H265Q LOX. Both wild-type and other mutant forms bound sulfite in reactions described by second-order kinetics, but H265Q displayed saturation kinetics, with a high K_d value of 125 mM and a maximum rate of 0.65 S^{-1} of the two step reaction, A + B ⇔ C -> D.

Spectral characterization of H265Q LOX

Both the peak position and the shape of the absorption spectra of H265Q LOX in near-UV and visible wavelength region were identical to that of the wild-type enzyme. The fluorescence spectrum of the active site FMN and the aromatic amino acid residues in H265Q were also similar to the wild-type enzyme. However, the circular dichroism (CD) spectrum of this mutant around 455 nm had less CD intensity than that for the wild-type enzyme (Fig.1). These results indicate that the imidazole ring of His-265

Table 1. Kinetic Parameters for Reductive, Oxidative, Sulfite-binding and Sulfite-releasing Reactions of Wild-type and Mutant Forms of LOX

	$k_{red}^{L\text{-}lac}$ ($M^{-1}s^{-1}$)	k_{ox}^{O2} ($M^{-1}s^{-1}$)	k_{on}^{SO3} ($M^{-1}s^{-1}$)	k_{off}^{SO3} (s^{-1})
H265Q	**0.01**	**$3.4x10^5$**	*** 5.3** (0.58 s^{-1}, 109 mM)	***n.d.***
Wild type	*** $8.0x10^5$** (520 s^{-1}, 0.67 mM)	**$1.8x10^6$**	**$1.8x10^5$**	**0.092**
R181K	*** $3.5x10^3$** (26 s^{-1}, 7.3 mM)	**$9.0x10^5$**	**$7.9x10^3$**	**0.0025**
R181M	*** 25** (2.3 s^{-1}, 94 mM)	**$8.0x10^4$**	**142**	**0.0032**
Fresh R268K	**210**	**$3.6x10^5$**	**$7.7x10^3$**	**0.0032**
R268M	**0.25**	**$1.3x10^5$**	**270**	**0.004**
R181K:R268K	**0.11**	**$2.9x10^5$**	**115**	**0.0025**

* The calculated value of k/Km; n.d., not determined

residue perturbs the electronic structure of the active site FMN, especially the electronic dipole moment that is oriented in the long axis of the isoalloxazine ring. Reduction by xanthine/xanthine oxidase or by glycine/light occurred similarly to wild-type and other mutant forms of enzyme, and indicated that an anionic semiquinone form is stable only under anaerobic circumstances.

Discussion

Replacing His-265 residue of wild-type LOX to Gln caused the instability of the Michaelis complex with L-lactate and decreased the rate of the reductive half-reaction of LOX with L-lactate by 10^8-fold. The rate of formation of the complex with sulfite was decreased by 10^4-fold, but the re-oxidation rate of the reduced form of enzyme with oxygen was decreased only 5-fold. Analogous mutations of other family members include the H290Q variant of L-lactate monooxygenase, and the H373Q mutant of flavocytochrome b_2, which had k_{cat} values that were decreased by 10^7-10^8 fold and 5 x 10^5 fold, respectively (*15,16*). Other mutations, including H274G, H274A, and H274D of L-mandelate dehydrogenase, resulted in completely inactive enzymes (*17*).

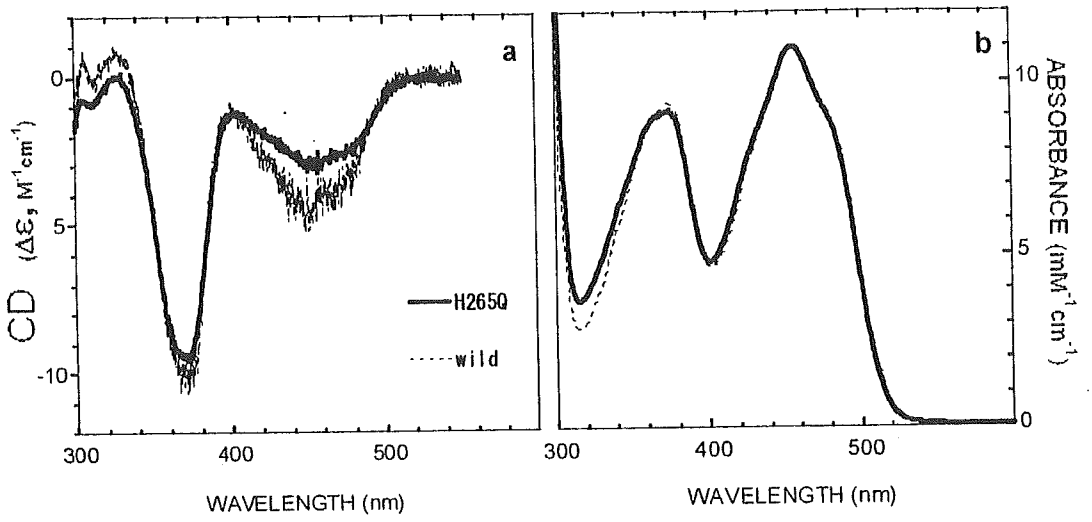

Fig. 1 Circular dichroism (*a*) and absorption (*b*) spectra of H265Q (*bold line*) and wild-type (*thin line*) L-lactate oxidase in 0.1 M sodium phosphate buffer, pH 7.0, at 25 °C.

The mutation of His-265 to glutamine also decreased the CD intensity at 455 nm compared to that of wild-type, while the CD intensity at 370 nm was almost unchanged.Other mutant forms where Arg-181 and/or Arg-268 were replaced by Lys or Met did not cause any changes in the CD at 455 nm (unpublished data). Our crystal structure analysis of wild-type LOX confirmed that the imidazole ring of His-265 stacked withthe FMN isoalloxazine-ring and had the lowest B-factor value of the conserved amino acid residues near the FMN (*unpublished data*). A closely related flavoprotein family consists of the FAD enzymes catalyzing the oxidative deamination of amino acids, such as D-amino acid oxidase (DAO), which has been well characterized both in function and in structure. The crystal structure of pig DAO was reported to have an active site that was a mirror-image of that of flavocytochrome b_2, although no homologous His residues were observed near FAD in the active site of DAO (*18*). These results demonstrate that the importance of His-265 in the active site lies in the binding and activation of the substrate by its interaction with FMN in the α-hydroxy acid enzyme family.

Acknowledgements
This work was supported by the United States Public Health Service Grant GM 11106 (to V.M. and D.P.B.)

References

1. Lederer, F. (1991) In: Chemistry and biochemistry of flavoenzymes, Vol. 2 (Muller F. ed.) CRC Press, Boca Raton, FL., *pp*153-242
2. Ghisla, S. & Massey, V. (1991) In: Chemistry and biochemistry of flavoenzymes, Vol. 2 (Muller F. ed.) CRC Press, Boca Raton, FL., *pp*243-289
3. Lindqvist, Y. & Branden, C.I. (1989) *J. Biol. Chem.* **264**, 3624-3628.
4. Le, K.H.D. & Lederer, F. (1991) *J. Biol. Chem.* **266**, 20877-20881.

5. Smekal, O., Yasin, M., Fewson, C.A., Reid, G.A. & Chapman, S.K. (1993) *Biochem. J.* **290**, 103-107
6. Xia, Z.X. & Mathews, F.S. (1990) *J. Mol.Biol.* **212**, 837-863.
7. Lindqvist, Y. (1989) *J. Mol. Biol.* **209**, 151-166.
8. Sukumar , N., Xu, Y., Gatti, D.L., Mitra, B. & Mathews, F.S. (2001) *Biochemistry* **40**, 9870-9878.
9. Cunane, L.M., Barton, J.D., Chen, Z-w, Le, K.H.D., Amar, D, Lederer F. & Mathews, F.S. (2001) *Biochemistry* **44**, 1521-1531.
10. Maeda-Yorita, K., Aki, K., Sagai, H, Misaki, H., & Massey, V. (1995) *Biochimie* **77**, 631-642.
11. Yorita, K, Matsuoka, T., Misaki, H. & Massey, V. (2000) *Proc. Natl. Acad. Sci. USA* **97**, 13039-13044.
12. Imai, Y., Matsushima, Y., Sugimura, T. & Terada, M. (1991) *Nucl. Acids Res.* **19**, 2785
13. Yorita, K, Aki, K., Ohkuma-Soejima, T., Kokubo, T. & Massey, V. (1996) *J. Biol. Chem.* **271**, 28300-28305.
14. Yorita, K, Janko, K., Aki, K., Ghisla, S., Palfey, B. & Massey, V. (1997) *Proc. Natl. Acad. Sci. USA* **94**, 9590-9595.
15. Muh, U., Williams, C.H., Jr., & Massey, V. (1994) *J. Biol. Chem.* **269**, 7989-7993.
16. Gaume, B., Sharp, R.E., Manson, F.D.C., Chapman, S.K., Reid, G.A. & Lederer, F. (1995) *Biochimie* **77**, 621-630.
17. Lehoux, I.E. & Mitra, B. (1999) *Biochemistry* **38**, 9945-9955.
18. Mattevi, A., Vanoni, M.A., Todone, F., Rizzi, M., Teplyakov, A., Coda, A., Bolognesi, M. & Curti, B. (1996) *Proc. Natl. Acad. Sci. USA* **93**, 7496-7501.

Acta Crystallographica Section F
Structural Biology and Crystallization Communications
ISSN 1744-3091

Crystallization and preliminary X-ray diffraction study of L-lactate oxidase (LOX), R181M mutant, from *Aerococcus viridans*

Yasufumi Umena,[a,b] Kazuko Yorita,[c] Takeshi Matsuoka,[d] Makoto Abe,[a] Akiko Kita,[a,e] Kiyoshi Fukui,[c] Tomitake Tsukihara[b] and Yukio Morimoto[a,e]*

[a]Research Reactor Institute, Kyoto University, Kumatori, Osaka 590-0494, Japan, [b]Institute for Protein Research, Osaka University, Suita, Osaka 565-0871, Japan, [c]Institute for Enzyme Research, The University of Tokushima, Tokushima 770-8503, Japan, [d]Fine Chemicals and Diagnostics Division, Asahi Kasei Pharma, Shizuoka 410-2321, Japan, and [e]RIKEN Harima Institute at Spring-8, Kohto, Mikazuki, Hyogo 679-5148, Japan

Correspondence e-mail: morimoto@rri.kyoto-u.ac.jp

Received 6 December 2004
Accepted 22 March 2005
Online 1 April 2005

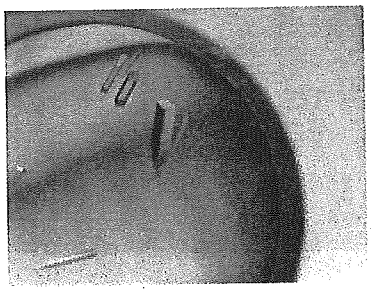

L-Lactate oxidase (LOX) from *Aerococcus viridans* is a member of the α-hydroxyacid oxidase flavoenzyme family. An X-ray crystallographic study of a LOX mutant in which Arg181 is replaced by Met was initiated in order to understand the functions of the conserved amino-acid residues around the FMN in the enzyme active site. LOX-R181M crystals belong to the tetragonal space group $I422$, with unit-cell parameters $a = b = 192.632$, $c = 200.263$ Å, $\alpha = \beta = \gamma = 90°$. There are four monomers in the asymmetric unit. Diffraction data were collected under cryogenic conditions to 2.44 Å resolution from LOX-R181M crystals at BL41XU, SPring-8.

1. Introduction

The α-hydroxyacid oxidases are a group of flavoproteins that catalyze the flavin mononucleotide (FMN) dependent oxidation of their respective substrates. These enzymes have been found to share remarkable similarities in catalytic properties and common structural motifs, making it likely that they constitute a family. The known members of this family are lactate dehydrogenase (flavocytochrome b_2; Lederer, 1991), L-lactate monooxygenase (Ghisla & Massey, 1991), glycolate oxidase (Lindqvist & Branden, 1989), L-mandelate dehydrogenase (Mitra *et al.*, 1993) and long-chain α-hydroxyacid oxidase (Diep Lê & Lederer, 1991). Within the family, the crystal structures of glycolate oxidase (Lindqvist, 1989), flavocytochrome b_2 (Xia & Mathews, 1990) and a chimeric form of L-mandelate dehydrogenase (Sukumar *et al.*, 2001) have been solved by X-ray diffraction studies. Comparison of these structures reveals similar protein-folding patterns, with each monomeric unit consisting of eight α-helices and eight β-strands in a typical α/β-barrel arrangement and with the FMN prosthetic group located at the C-terminal end of the β-strands.

L-Lactate oxidase (LOX) from *Aerococcus viridans* catalyzes the oxidation of L-lactate using molecular oxygen with the formation of pyruvate and H_2O_2 as products (Maeda-Yorita *et al.*, 1995). We previously reported the crystallization of the wild-type enzyme, but the quality of the crystals was not sufficient to solve the structure (Morimoto *et al.*, 1998). The reaction mechanisms and substrate specificities of the α-hydroxyacid oxidases are based on the interactions of FMN and the respective substrates with the adjacent amino-acid residues at the active sites. Therefore, determination of the three-dimensional structure of LOX is an important step to facilitate more detailed mechanistic studies of these flavoenzymes.

Two Arg residues in LOX, Arg181 and Arg268, are conserved in all the α-hydroxyacid oxidase family members. Based on the X-ray crystal structures of glycolate oxidase and flavocytochrome b_2, these two Arg residues are located in the vicinity of the FMN and are likely to be part of the substrate-binding site. We produced the site-directed mutant LOX-R181M, with Arg181 replaced by Met, in order to determine the effect of removing the positive charge at this position (Yorita *et al.*, 2000). In LOX-R181M, there were only small effects on the reactivity of the reduced FMN with oxygen, but the efficiency of reduction of oxidized FMN by L-lactate was greatly reduced (Yorita *et al.*, 2000). These results demonstrated the participation of Arg181 both in the binding of the substrate L-lactate and in influencing the

doi:10.1107/S1744309105009152

properties and reactivity of the active-site FMN. Here, we describe the crystallization of LOX-R181M and preliminary X-ray diffraction results.

2. Materials and methods

2.1. Crystallization

Expression and purification of the LOX-R181M mutant has been described in previous reports (Maeda-Yorita *et al.*, 1995; Yorita *et al.*, 2000). The enzyme was passed through a Sephacryl S-200HR (Amersham Biosciences) column prior to crystallization and was then concentrated to 20 mg ml^{-1} in 50 m*M* Tris buffer pH 8.0 using a Centricon YM-10 (Millipore). The protein concentration was determined using a molecular-extinction coefficient at 456 nm of 11.0 × 10^3 *M*$^{-1}$ cm^{-1}; the protein has a molecular weight of 40 865 Da (Maeda-Yorita *et al.*, 1995).

Wild-type LOX was previously crystallized at 288 K from a solution containing 10%(*w*/*v*) polyethylene glycol (PEG) 6000, 100 m*M* MES buffer pH 6.0 at a protein concentration of 16 mg ml^{-1} (Morimoto *et al.*, 1998). We tried to crystallize LOX-R181M under the same conditions, but the result was only very thin crystals that were not suitable for diffraction experiments. We expanded crystallization trials of LOX-R181M around the original condition used to crystallize the wild-type enzyme by varying the PEG size, PEG concentration and buffer pH. One of the crystal optimization trials is shown in Fig. 1(*a*). In addition, we used the Additive Screen kit (Hampton Research) with either the hanging-drop or sitting-drop vapour-diffusion methods at 298 K. 1 µl of each additive solution was mixed with 4 µl reservoir solution; 2 µl protein solution and 2 µl of this premixed solution were then combined to form the crystallization drop. After optimization using the additive reagents, we found benzamidine–HCl to be the most effective additive reagent. Single crystals suitable for X-ray diffraction experiments were grown at 298 K using a reservoir solution consisting of 18–20%(*w*/*v*) PEG 8000 and 50 m*M* Tris buffer pH 8.0 and an additive solution consisting of 2%(*w*/*v*) benzamidine–HCl. The final volume of the reservoir solution was

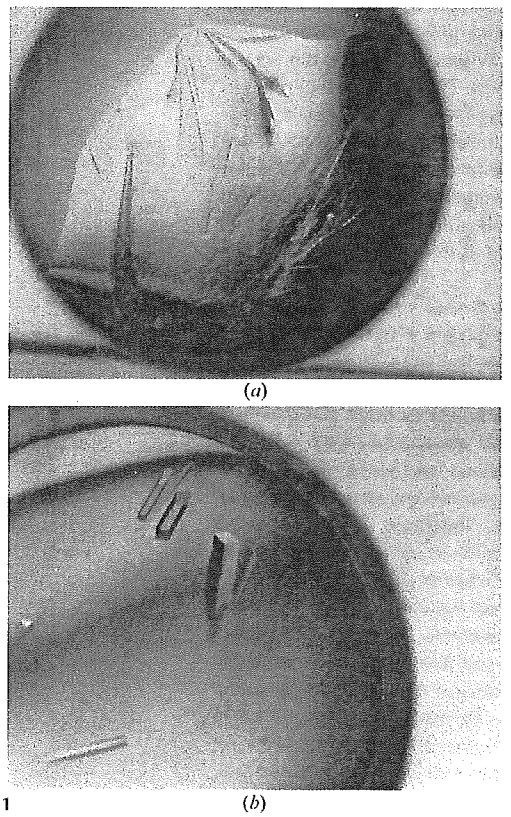

(*a*)

(*b*)

Figure 1
Crystals of the LOX-R181M mutant appear yellow owing to the presence of FMN. The crystals were grown in a solution containing 20%(*w*/*v*) PEG 8000 and 50 m*M* Tris buffer pH 8.0 (*a*) in the absence and (*b*) in the presence of 2% benzamidine–HCl. The dimensions of the rod-shaped crystals are approximately 0.3 × 0.1 × 0.1 mm.

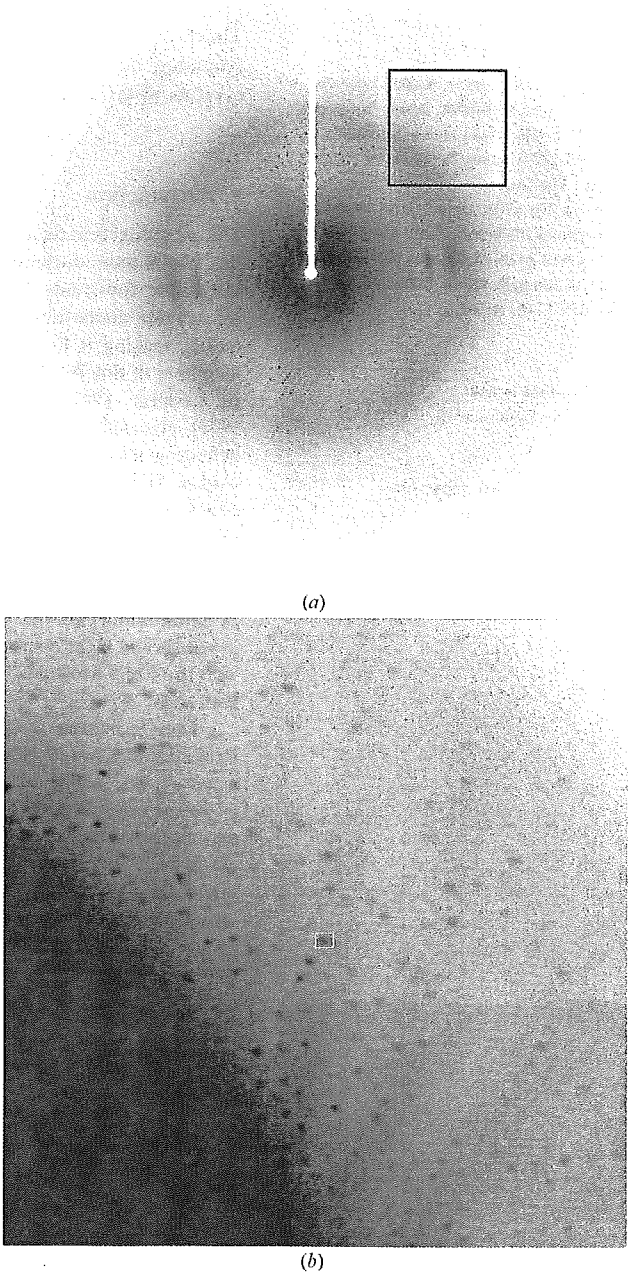

(*a*)

(*b*)

Figure 2
A typical diffraction pattern for a LOX-R181M crystal with high-angle reflections. (*a*) Normal size, (*b*) enlargement of the square in (*a*) near 2.5 Å resolution.

Table 1
Crystal parameters and data-collection statistics.

Values in parentheses are for the effective highest resolution shell (2.69–2.44 Å).

Space group	*I*422
Unit-cell parameters (Å, °)	a = 192.632, b = 192.632, c = 200.263, α = 90, β = 90, γ = 90
Resolution (Å)	2.44
Crystal-to-detector distance (mm)	130
Wavelength (Å)	1.000
Exposure time (s)	5.0
No. of measurements	1745892
No. of unique reflections	103478
Redundancy	10.8
R_{sym}† (%)	13.7 (32.7)
Completeness (%)	94.3 (100.0)
$I/\sigma(I)$	3.6 (2.2)

† $R_{sym} = \sum_{hkl}\sum_i |I_i(hkl) - \langle I(hkl)\rangle| / \sum_{hkl}\sum_i I_i(hkl)$, where $I_i(hkl)$ are the intensities of symmetry-related reflections and $\langle I(hkl)\rangle$ is the average intensity over all symmetry equivalents.

200 µl. In the presence of benzamidine–HCl, we obtained large single intensely yellow rod-shaped crystals with dimensions of approximately 0.3 × 0.1 × 0.1 mm (Fig. 1*b*).

2.2. Data collection

A crystal was mounted in a cryoloop and flash-frozen in a nitrogen-gas stream at 100 K. X-ray diffraction data were collected with a MAR CCD detector using synchrotron radiation at beamline BL41XU of SPring-8, Japan. The synchrotron wavelength was 1 Å and the crystal-to-detector distance was maintained at either 200 or 130 mm. A total of 180 frames were collected with 1° oscillation and 5 s exposures. A typical diffraction pattern is shown in Fig. 2 with high-angle reflections. The data were collected to 2.44 Å resolution and were processed with the program *HKL*2000 (Otwinowski & Minor, 1997). The data-collection statistics are given in Table 1.

3. Results and discussion

We have successfully obtained large diffracting crystals of LOX-R181M and collected a complete data set under cryogenic conditions using the SPring-8 synchrotron facility. Since LOX-R181M crystals grow in the presence of benzamidine, we were able to concentrate the crystallization drop by evaporation and then use this solution as a cryoprotectant. After the LOX-R181M crystals had grown to full size, the hanging- or sitting-drop well in the crystallization box was opened and the drop solution was allowed to evaporate gradually. At 5 min intervals during the evaporation procedure, a small amount of the solution was scooped into a cryo-mounting loop and the diffraction pattern was checked for ice rings. This evaporation procedure was successful in cryoprotecting the LOX-R181M crystal for the diffraction experiment.

Crystals of the LOX-R181M mutant belong to the tetragonal space group *I*422, with unit-cell parameters $a = b = 192.632$, $c = 200.263$ Å. Considering the molecular weight of the LOX-R181M mutant (40 842 Da), we assume there to be four LOX-R181M monomers in an asymmetric unit and thus 64 monomers in a unit cell, resulting in a Matthews coefficient (V_M) of 2.81 Å^3 Da^{-1} and a solvent content of 56.1%. These values are in the normal range for globular protein crystals (Matthews, 1968; Kantardjieff & Rupp, 2003).

Glycolate oxidase (GLO) crystallized in space group *I*422, in which the crystal packing of GLO yields an octamer (Lindqvist & Branden, 1989). Molecular-exclusion chromatography of lactate oxidase using Sephadex G-100 provided the basis for the report that wild-type LOX was a tetramer in 50 m*M* potassium phosphate buffer pH 7.0 in the presence of 0.2 *M* potassium chloride (Duncan *et al.*, 1989). Thus, our LOX-R181M crystals may contain four monomers in the asymmetric unit.

Molecular-replacement analysis of LOX-R181M using the program *CNS* (Brünger *et al.*, 1998) with the glycolate oxidase molecule (PDB code 1gox; Lindqvist, 1989) as a search model is now under way to solve the structure. Crystallization trials of wild-type LOX and new LOX mutants are also in progress with and without substrate or substrate analogues using the same methods that were successful for the R181M mutant.

This research was partly supported by a Grant-in-Aid (to YM) for the National Project on Protein Structural and Function Analysis from the Ministry of Education, Culture, Sports, Science and Technology of Japan, for which the authors are greatly appreciative.

References

Brünger, A. T., Adams, P. D., Clore, G. M., DeLano, W. L., Gros, P., Grosse-Kunstleve, R. W., Jiang, J.-S., Kuszewski, J., Nilges, M., Pannu, N. S., Read, R. J., Rice, L. M., Simonson, T. & Warren, G. L. (1998). *Acta Cryst.* D**54**, 905–921.
Diep Lê, K. H. & Lederer, F. (1991). *J. Biol. Chem.* **266**, 20877–20881.
Duncan, J. D., Wallis, J. O. & Azari, M. R. (1989). *Biochem. Biophys. Res. Commun.* **164**, 919–926.
Ghisla, S. & Massey, V. (1991). *Chemistry and Biochemistry of the Flavoenzymes*, Vol. 2, edited by F. Muller, pp. 243–289. Boca Raton, FL, USA: CRC Press.
Kantardjieff, K. A. & Rupp, B. (2003). *Protein Sci.* **12**, 1865–1871.
Lederer, F. (1991). *Chemistry and Biochemistry of the Flavoenzymes*, Vol. 2, edited by F. Muller, pp. 153–242. Boca Raton, FL, USA: CRC Press.
Lindqvist, Y. (1989). *J. Mol. Biol.* **209**, 151–166.
Lindqvist, Y. & Branden, C. I. (1989). *J. Mol. Biol.* **264**, 3624–3628.
Maeda-Yorita, K., Aki, K., Sagai, H., Misaki, H. & Massey, V. (1995). *Biochimie*, **77**, 631–642.
Matthews, B. W. (1968). *J. Mol. Biol.* **33**, 491–497.
Mitra, B., Gerlt, J. A., Babbitt, P. C., Koo, C. W., Kenyon, G. L., Joseph, D. & Petsko, G. A. (1993). *Biochemistry*, **32**, 12959–12967.
Morimoto, Y., Yorita, K., Aki, K., Misaki, H. & Massey, V. (1998). *Biochimie*, **80**, 309–312.
Otwinowski, Z. & Minor, W. (1997). *Methods Enzymol.* **276**, 307–326.
Sukumar, N., Xu, Y., Gatti, D. L., Mitra, B. & Mathews, F. S. (2001) *Biochemistry*, **40**, 9870–9878.
Xia, Z. X. & Mathews, F. S. (1990). *J. Mol. Biol.* **212**, 837–863.
Yorita, K., Matsuoka, T., Misaki, H. & Massey, V. (2000). *Proc. Natl Acad. Sci. USA*, **97**, 13039–13044.

D-アミノ酸代謝システムによる脳機能制御の医化学

岩名沙奈恵
Sanae IWANA
徳島大学分子酵素学研究センター
遺伝制御学部門大学院生

福井　清
Kiyoshi FUKUI
徳島大学分子酵素学研究センター
遺伝制御学部門教授

1 はじめに

生体に存在するアミノ酸には2種類の光学異性体，L型とD型が存在する．このうち，生体内に豊富に存在するタンパク質を構成するのはL型のアミノ酸のみであり，D型アミノ酸は生体には存在しないと考えられてきた．しかし近年，D型アミノ酸に関する発見と研究が進み，生体にD型アミノ酸が存在し，生体機能の維持・調節機構に積極的に関与していることが明らかになってきている．

生体内における役割が明確になってきたD-アミノ酸の例としては，D-アスパラギン酸及びD-セリンが挙げられる．D-アスパラギン酸は松果体においてメラトニンの合成・分泌を抑制し，精巣においてはテストステロンの合成・分泌を促進することが判明している.[1,2] またD-セリンに関しては，中枢神経系におけるNMDA(*N*-methyl-D-aspartate)受容体のグリシン結合部位における内因性結合物質として神経伝達の調節に関与していることが明らかとされている.[3]

本稿では，当研究室が解析の中心に据えているD-アミノ酸酸化酵素(D-amino acid oxidase；DAO)とその内在性基質と考えられるD-セリンを中心として，脳機能制御におけるD-アミノ酸代謝システムについて，その概要を紹介する．

2 D-セリンによるNMDA受容体の機能調節

中枢神経系においては，D-セリンが高濃度に存在し，その脳内分布はNMDA受容体の分布と正の相関性を示すことが報告されている.[4] NMDA受容体は，イオンチャネルを内蔵し速い神経伝達を担う，チャネル型グルタミン酸受容体のサブタイプであり，興奮性神経伝達，シナプス可塑性，並びに記憶・学習といった高次脳機能に重要な働きを担っている．NMDA受容体の過興奮は細胞内へのカルシウムイオン流入の増大を招き，脳卒中，神経変性疾患等様々な脳の病態における神経細胞死に関与している可能性が指摘されている.[5]

NMDA受容体は興奮性神経伝達物質であるL-グルタミン酸の結合部位の他にグリシンの結合部位を有し，グリシンの結合はNMDA受容体の活性化に必須である．NMDA受容体のグリシン結合部位にはD-セリンがアゴニストとして結合しうる．また，グリシン結合部位に対するアンタゴニストは，脳卒中モデル動物において神経保護作用を有することが報告されている.[6] 一方，脳卒中後の血液再環流時にD-セリン，グリシンの細胞外レベルが上昇しているとの報告もある.[7] これらのことは，調節因子の上昇がNMDA受容体の過興奮による神経細胞毒性に関与していることを示唆するものであると考えられる．以上のことからD-セリンが，脳においてNMDA受容体のグリシン結合部位における内在性の神経伝達調節因子として働き，NMDA受容体の活性制御に関与しているということが予想される．また，セリンのラセミ化を触媒し，L-セリンからD-セリンの生合成を司ると考えられる酵素，セリンラセマーゼもマウス脳において単離同定されている.[8]

3 D-セリン代謝とD-アミノ酸酸化酵素

一方，D型のアミノ酸のみを特異的に代謝する酵素DAOの歴史は古く，1935年にクエン酸回路の発見者Krebsによって報告されたことに始まる．DAOはflavin adenine dinucleotide(FAD)(ビタミンB2誘導体)を補酵素として活性中心に持つフラビン酵素であり，生体内でのDAOの発現は脳，腎臓，腸管，肝臓において認められている．800種近くあるフラビン酵素のなかでも，最も初期に発見されたFAD酵素の1つであり，その酵素学的諸性質については詳細な解析がなされてきた．DAOはD-アミノ酸のうち，中性及び芳香族性のものを良い基質とするが，グリシンも基質となりうる．

一方で，D-アミノ酸を特異的に代謝するDAOの生体における役割は長い間不明であった．しかし，約10年前に中枢神経系における遊離D-セリンが同定され，さらにその中枢神経系における分布がNMDA受容体の分布と一致することが報告された．さらにD-セリンがNMDA受容体のグリシン結合部位におけるアゴニストであることが明らかにされたことから，「D型アミノ酸による神経伝達調節機構」という新たな概念における，脳内D-セリンの存在意義が示された．これらの知見により，DAOがD-セリン代謝への関与を通じてNMDA受容体を介した脳機能維持に積極的に貢献していることが示唆されるに至った．

当研究室では，DAOの生体における役割及び分子レベル・細胞レベルでの活性制御メカニズムの解析が，NMDA受容体機能異常・機能低下に伴う難治性精神疾患等の病態解明や新規治療薬開発へつながるとの考えに基づき，研究を行っている．

4 D-アミノ酸酸化酵素の諸性質と生体における意義

DAOは分子量40 kDaほどのタンパク質で，約350アミノ酸残基からなる．C末端に3残基のアミノ酸Ser-His-Leuから成るペルオキシゾーム移行シグナル(PTS 1；peroxisome targeting signal 1)を有し，細胞内で成熟タンパク質として合成された後，プロセシングは受けずに細胞内小器官のひとつで脂肪酸代謝や種々の分子の解毒に関与するペルオキシゾームへ移行，局在する．

DAOの触媒反応は補酵素FADの酸化還元状態に基づいて2つのステップに分けられる．以下の反応式と図1で示したように，本酵素によって基質は酸化的脱アミノ反応を受け，1分子のアンモニアと過酸化水素が発生する．

$$RCHNH_2COOH + DAO \cdot FAD \rightleftarrows RC=NHCOOH + DAO \cdot FADH_2 \quad (式1)$$

$$RC=NHCOOH + H_2O \rightleftarrows RCOCOOH + NH_3 \quad (式2)$$

$$DAO \cdot FADH_2 + O_2 \rightarrow DAO \cdot FAD + H_2O_2 \quad (式3)$$

触媒反応は基質であるD-アミノ酸からFADに2電子が移行する還元的半反応(式1)，続いて還元型FADが酸素分子を2電子還元し過酸化水素が発生する酸化的半反応(式3)によって進行する．生じた過酸化水素はペルオキシゾーム内でカタラーゼ等によって加水分解されると考えられる．これら2つのステップは基質代謝における1サイクルであり，酸化型FADに新たな基質分子が反応することで次のサイクルが開始する．FADとDAOタンパクとの結合は非共有結合であり，したがってその結合は比較的弱い．DAOのFAD取り込みは，翻訳時もしくは翻訳後のいずれかの段階において起こると考え

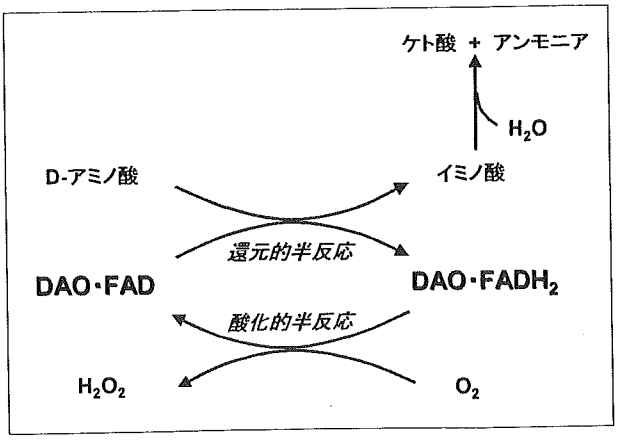

図1 DAOによるD-アミノ酸代謝の模式図

還元的半反応において，FADは基質を酸化し還元型となる．続く酸化的半反応では，還元型FADが酸素分子を還元し過酸化水素を発生させる．この2つのステップを経て，FADはもとの酸化型へ戻り，次なる基質分子と反応する．DAOが触媒するのはイミノ酸形成までである．イミノ酸は非酵素的加水分解によりケト酸とアンモニアを生ずる．

られる．過酸化水素の発生という観点からみると，DAOが外来感染源に対する免疫面において何らかの役割を有している可能性が考えられる．[9] さらにDAO機能亢進や基質過剰状態により過剰発生した過酸化水素は，細胞に対する酸化ストレスとなり，細胞死を誘導しうる．この点からは抗腫瘍効果が期待されている．[10]

一方，還元的半反応において酸化されたD-アミノ酸はイミノ酸となり，直ちに非酵素的な加水分解を受けてα-ケト酸とアンモニアとなる(式2)．生じたα-ケト酸は，図2に示したように細胞質においてアミノ酸に再利用されると考えられる．D-アミノ酸の生体における役割が知られていなかった頃，食物摂取等によって取り込まれた外来性のD-アミノ酸はL-アミノ酸を合成する「材料」であると考えられていた．図2に示したものは，かつて古武弥四郎先生が提唱されたstereonaturalisationという概念であり，Krebsが報告したDAOによるD-アミノ酸からのケト酸の生成とBraunsteinが報告したアミノ基転移酵素によるケト酸からのL-アミノ酸の生成の両者を合わせて，D-アミノ酸からL-アミノ酸への1つの流れが存在することを示したものである．近年，生体内でD-アミノ酸が合成され独自の機能を有するということが分かってきたため，この機構はD-アミノ酸の代謝分解・濃度調節に関わる経路の1つとして捉えることができる．脳におけるセリンラセマーゼの発見は，この逆方向の反応も生体内で機能していることを示唆するものと考えられる．

脳においてDAOとD-セリンの分布は負の相関性を示す．当研究室ではラット脳由来グリア細胞培養系を用い，DAOの遺伝子発現を小脳のみならず従来は否定的であった大脳由来グリア細胞においても確認した．さらにタイプⅠ，Ⅱアストロサイトの分離培養法を確立し，これによってタイプⅠアストロサイトにおいてDAO発現が顕著であることを明らかとした．[11] 一方，D-セリン産生の場はタイプⅡアストロサイトであると報告されている．[3] また，DAOを強制発現させたラットのアストロサイトを用いてD-セリン投与の影響を調べた結果，DAOがD-セリンの代謝に積極的に関与していることが示唆された(未発表)．これらの知見をモデル化したものが図3である．

神経疾患における*DAO*遺伝子変異の解析は，以前から興味深い課題であった．1995年に12番染色体上の*DAO*ゲノム遺伝子内に存在するマイクロサテライトマーカーの解析から，我々は2型脊髄小脳変性症の病因遺伝子が*DAO*遺伝子近傍1 centi Morgan*に存在することを報告した．[12] また，近年ゲノムSNPs解析の結果から統合失調症疾患感受性遺伝子の1つとしてDAOが報告され，その統合失

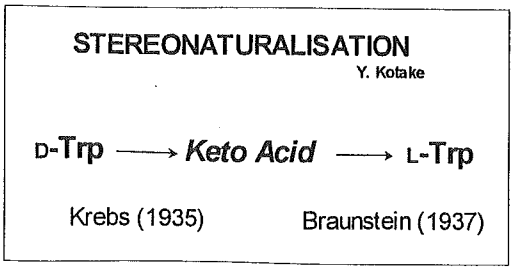

図2　D-アミノ酸からL-アミノ酸への変換

D-アミノ酸はケト酸を経由してL-アミノ酸に再利用されると考えられる．D-アミノ酸はDAOによって代謝された後，加水分解を経てケト酸となる．このケト酸はL-アミノ酸生合成の原材料となる．

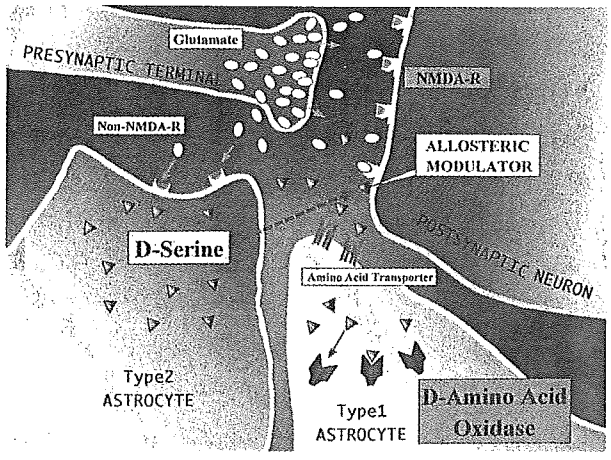

図3　中枢神経系「DAO・D-セリンシステム」

DAO・D-セリンによるNMDA受容体の調節機構をモデル図で示した．DAOによるD-セリン代謝の場はタイプⅠアストロサイト，D-セリン産生の場はタイプⅡアストロサイトであると考えられる．シナプス間隙の遊離D-セリンは，NMDA受容体のグリシン結合部位におけるアロステリック調節因子として作用し，グルタミン酸と共にNMDA受容体を介する神経伝達に関与する．

＊　Morganについての用語解説は，846頁参照．

調症との関連が示唆された.[13] この発見は，DAO活性の上昇がD-セリン代謝亢進を介してNMDA受容体の機能を低下させ，統合失調症の発症に至るとする仮説を裏付けるものであった．統合失調症遺伝子解析の結果からは，同時に新規遺伝子である*G72*も疾患感受性遺伝子として発見され，yeast two hybrid法を用いた実験により，G72遺伝子産物とDAOは相互作用することが報告された.[13]

さらに組換えタンパク質を用いた*in vitro*の実験からG72タンパクがDAOの活性を上昇させることも示された．G72タンパクによるDAOの活性上昇は，DAOによるD-セリン代謝亢進を招き，シナプス間隙のD-セリン濃度の減少によるNMDA受容体の機能低下を引き起こして，統合失調症の病態に関与すると考えられる．G72の遺伝子産物との相互作用によるDAO活性制御の詳細とその病態生理学的意義についてはまだ解明されておらず，今後の重要な研究課題であると考えられる．

5 統合失調症と神経伝達系の異常

統合失調症(旧精神分裂病)は有病率1%の比較的頻度の高い疾患であるが，人的経済的コスト面で人類のかかる最悪の疾患の1つであるとされる．男女間で有病率に差はないが，発症のピークは，男性が20歳前後であるのに対し，女性は20歳代後半から40歳代と違いがみられる．一親等に統合失調症患者がいる場合や一卵性双生児で片方が統合失調症患者の場合，発症するリスクは前者で約15%，後者では50%以上である．診断学的には陽性症状(妄想・幻覚，精神運動興奮等)，陰性症状(情動の平板化，社会的引きこもり等)の2症状に分けられ，患者はこれらの症状の片方のみか，もしくは両方の症状を呈す．一般的に，陰性症状に比べて陽性症状のほうが薬物治療に対する反応性が良好である．統合失調症の症状によって，機能遂行力，社交性といった患者の社会的能力が障害される．

統合失調症は多因子疾患であり，遺伝素因と環境因子の両方が発症に関与するとされているが，その発症と病態の病理学的メカニズムは未だ仮説の域を出ない．幾つかの神経伝達系の異常(ドパミン説，セロトニン説，NMDA受容体機能低下説など)が仮説として提唱されており，単一のみならず複数の神経伝達系の機能異常が統合失調症の多様な病態を形成していると考えられる．これらのなかでD-セリンの直接的関与が示唆された伝達系が，先に述べたNMDA受容体を介する神経伝達系である．

NMDA受容体アンタゴニスト服用やNMDA受容体発現減少により統合失調症様症状が誘発されることは以前から知られている．このことはNMDA受容体機能低下説の根拠の1つとなっており，NMDA受容体の機能改善は統合失調症の病状の改善につながると考えられる.[14,15] 統合失調症様症状発現薬(NMDA受容体アンタゴニスト)による動物の異常行動がD-セリン投与で抑制されることや，統合失調症患者の薬物治療にNMDA受容体のアゴニストであるグリシンやD-セリン，または抗結核剤であり，NMDA受容体のグリシン結合部位においては部分アゴニストとして働くD-サイクロセリンを加えることで治療効果が高まることなどから，NMDA受容体を介する神経伝達異常にD-セリンレベルの異常が関与している可能性は高いと考えられる.[15~17] そこで当研究室では，脳においてD-セリンの代謝を担う酵素としてDAOを位置付け，DAOの機能亢進によりD-セリン代謝が亢進すると，シナプス間隙の遊離D-セリン濃度の減少を介してNMDA受容体の機能が低下し，統合失調症をはじめとする精神疾患を引き起こすとの仮説を提唱している．DAOと統合失調症との関係はゲノム解析のみから示唆されたものであり，タンパク質レベルでの解明には未だ至っていないため，現在解析を進めているところである．

6 脳内D-アミノ酸制御システムの今後

D-セリンの豊富な，前脳の健常状態におけるDAOの発現は，現在までのところ初代培養グリア細胞の系で確認されているだけである.[11] 一方，D-セリンの生合成を司るセリンラセマーゼの脳内分布は，D-セリンの分布と正の相関性を有しており，前脳部に多く，脳幹にはごくわずかな発現が認められるのみである.[8] 最近になって，セリンラセマーゼがD-セ